Using synthetic tracers as a proxy for summertime $PM_{2.5}$ air quality over the Northeastern United States in physical climate models

Yuanyuan Fang,[1,2] Arlene M. Fiore,[3] Jean-François Lamarque,[4] Larry W. Horowitz,[5,6] and Meiyun Lin[5,6]

[1] Fine particulate matter ($PM_{2.5}$) is a criteria pollutant. Its sensitivity to meteorology implies its distribution will likely change with climate shifts. Limited availability of global climate models with full chemistry complicates efforts to assess rigorously the uncertainties in the $PM_{2.5}$ response to a warming climate. We evaluate the potential for $PM_{2.5}$ distributions in a chemistry-climate model under current-day and warmer climate conditions over the Northeastern United States to be represented by a Synthetic Aerosol tracer (SAt). The SAt implemented into the Geophysical Fluid Dynamics Laboratory chemistry-climate model (AM3) follows the protocol of a recent multimodel community effort (HTAP), with CO emissions, 25-day chemical lifetime, and wet deposition rate of sulfate. Over the Northeastern United States, the summer daily time series of SAt correlates strongly with that of $PM_{2.5}$, with similar cumulative density functions under both present and future climate conditions. With a linear regression model derived from $PM_{2.5}$ and SAt in the current-day simulation, we reconstruct both the current-day and future $PM_{2.5}$ daily time series from the simulated SAt. This reconstruction captures the summer mean $PM_{2.5}$, the incidence of days above the 24-h mean $PM_{2.5}$ NAAQS, and $PM_{2.5}$ responses to climate change. This reconstruction also works over other polluted Northern Hemispheric regions and in spring. Our proof-of-concept study demonstrates that simple tracers can be developed to mimic $PM_{2.5}$, including its response to climate change, as an easy-to-implement and low-cost addition to physical climate models that should help air quality managers to reap the benefits of climate models that have no chemistry.

All Supporting Information may be found in the online version of this article.
[1]Princeton University, Woodrow Wilson School of Public and International Affairs, Princeton, NJ, USA.
[2]Now at Department of Global Ecology, Carnegie Institution for Science, Stanford, CA, USA.
[3]Department of Earth and Environmental Sciences and Lamont-Doherty Earth Observatory of Columbia University, Palisades, NY, USA.
[4]National Center of Atmospheric Research, Atmospheric Chemistry Division and Climate and Global Dynamics Division, Boulder, CO, USA.
[5]NOAA Geophysical Fluid Dynamics Laboratory, Princeton, NJ, USA.
[6]Princeton University, Atmospheric and Oceanic Sciences Program, Princeton, NJ, USA.

Corresponding author: Y. Fang, Department of Global Ecology, Carnegie Institution for Science, Stanford, CA, USA. (yyfang@stanford.edu)

1. Introduction

[2] Fine particulate matter ($PM_{2.5}$) causes a variety of adverse health effects, resulting in increased mortality and hospital admissions for cardiovascular and respiratory diseases [*Dockery et al.*, 1993; *Pope*, 2000; *Pope et al.*, 2002; *Schwartz et al.*, 2002; *Pope and Dockery*, 2006; *Parry et al.*, 2007]. It is also responsible for a reduction in visibility [*Park et al.*, 2006] and changes in climate [*Parry et al.*, 2007; *Kloster et al.*, 2010]. In the United States, $PM_{2.5}$ is regulated under the Environmental Protection Agency's National Ambient Air Quality Standard (NAAQS) as a criteria air pollutant with a daily mean threshold of 35 $\mu g/m^3$ and an annual mean threshold of 15 $\mu g/m^3$. As the concentration of $PM_{2.5}$ is highly sensitive to meteorological conditions, it is expected to respond to climate change [*Jacob and Winner*, 2009; *Fiore et al.*, 2012]. Therefore, regardless of potential changes in precursor emissions, a thorough understanding of the effects of global climate change on $PM_{2.5}$ concentrations is central to future air quality planning. We show that implementing synthetic tracers into the current generation of climate models offers a powerful, simple, and computationally efficient approach to project climate-driven changes to air quality.

[3] Although previous studies project significant changes in $PM_{2.5}$ in a warming climate, uncertainties exist regarding even the sign of the change ($-0.1 \pm 10\,\mu g/m^3$) [*Jacob and Winner*, 2009]. Recent studies using coupled chemistry-climate models suggest an increase in $PM_{2.5}$ despite globally increasing precipitation, reflecting a reduction in large-scale precipitation over polluted regions and seasons [*Fang et al.*, 2011; *Kloster et al.*, 2010]. On the regional scale, changes of $PM_{2.5}$ in a warming climate are even more difficult to project due to uncertainties in regional boundary layer ventilation and precipitation [*Meehl et al.*, 2007]. As only a handful of climate models are available with fully coupled chemistry and computational constraints often limit chemical transport models to using a limited set of meteorology from a single climate model, a rigorous evaluation of the uncertainties in the $PM_{2.5}$ response to various climate change scenarios projected by a suite of climate models is challenging.

[4] Synthetic tracers have been applied previously within chemical transport models to advance our understanding of the source, transport, and removal processes for regional air pollution and hemispheric pollution transport [e.g., *Bey et al.*, 2001; *Staudt et al.*, 2001; *Stohl et al.*, 2002; *Liu et al.*, 2005; *Shindell et al.*, 2008; *HTAP*, 2007, 2010]. Synthetic tracers have also been used in climate models to estimate how changes in the atmospheric circulation and precipitation affect air quality [*Mickley et al.*, 2004; *Fang et al.*, 2011]. Over many regions, including the Northeastern United States, the day-to-day variability of $PM_{2.5}$, which is directly

related to pollution episodes, is strongly affected by synoptic transport processes [*Cooper et al.*, 2001; *Tai et al.*, 2012; *Appelhans et al.*, 2012], and wet removal dominates PM$_{2.5}$ loss [*Textor et al.*, 2006]. Therefore, it is important to include both transport and wet removal in the design of a synthetic tracer for PM$_{2.5}$. The Task Force on Hemispheric Transport of Atmospheric Pollution (HTAP) has designed a diagnostic tracer experiment (TP1x), consisting of a soluble tracer with CO emissions to compare aerosol simulations across models. We incorporate a similar diagnostic tracer into the Geophysical Fluid Dynamics Laboratory (GFDL) AM3 model and provide a proof-of-concept study that illustrates the potential of synthetic tracers to represent daily PM$_{2.5}$ statistics, including their changes in a warming climate.

2. Method

2.1. Model and Simulations

[5] We use simulations from the GFDL chemistry-climate model (AM3) for current-day (1981–2000) and future (2081–2100) climate conditions and PM$_{2.5}$ distributions as described by *Fang et al.* [2011]. Briefly, the simulations are designed to study the effect of climate change on pollutants in the absence of emission changes. We further aim to minimize "noise" from interannual variability in order to allow the "signal" from climate change to emerge in our simulations. Specifically, the current-day simulation is driven by a 1981–2000 climatology of observed monthly mean sea surface temperature and sea ice. The future simulation is driven by this observed climatology plus the 19-model (from IPCC AR4) ensemble mean difference of 20-year average values (applied separately for each month, ensemble model mean annual change in SST is shown in Figure S1 in the Supporting Information) from 1981–2000 to 2081–2100 under the SRES A1B scenario. The global mean surface temperature increase projected by the IPCC AR4 model ensemble is 2.8 K. Emissions of short-lived pollutants in both present and future simulations are set to 1990 levels, repeated annually. The concentrations of the long-lived greenhouse gases (CO$_2$, N$_2$O, and CFCs) are set to 1990 values for the present but 2090 (A1B) values for the future simulation. CH$_4$ is set to the 1990 level for tropospheric chemistry calculations in both simulations but to the 1990 and A1B 2090 level for radiation (climate forcing) in the current-day and future simulations, respectively. Each simulation is run for 20 years following a 1-year spin-up.

[6] As CO is considered a useful tracer of anthropogenic pollutants, *HTAP* [2010] proposed synthetic tracers with 25-day chemical lifetime that follow CO emissions (including anthropogenic and biomass burning emissions from the RETRO [*Schultz and Rast*, 2007] and GFED v2 [*van der Werf et al.*, 2006] inventories for 2001, respectively) to help diagnose the transport processes affecting air pollutant distributions. We use these emissions and follow the HTAP approach of implementing a soluble version of this tracer, with wet deposition rates as sulfate, for our Synthetic Aerosol tracer (SAt). The global lifetime of SAt is about 4–6 days depending on season, close to that of the major PM$_{2.5}$ components: the AEROCOM all-model-average annual lifetime is 4 days for SO$_4$ and dust and 6–7 days for primary organic matter and black carbon [*Textor et al.*, 2006]. In this study, we incorporate SAt into the AM3 simulations and examine its utility as a proxy for PM$_{2.5}$ air quality in physical climate models,

focusing mainly on the Northeastern United States. SAt does not have real chemistry; therefore, it is expected to work best for PM$_{2.5}$ components with little chemistry. Nevertheless, as we show in section 3, the capability of SAt to represent the daily variability of and climate change effects on PM$_{2.5}$ suggests that transport and wet deposition are the major drivers for the climate change effect and the daily variability.

2.2. Model Evaluation

[7] *Donner et al.* [2011] show that the AM3 simulated aerosol optical depth and co-albedo broadly capture those in AERONET observations (agreement within a factor of 2 at most sites, with a global correlation coefficient ranging from 0.6 to 0.7). As we focus here on air quality over the Northeastern United States in summer (June–July–August), we evaluate the surface PM$_{2.5}$ concentration (defined as the sum of sulfate, nitrate, dust with a dry radius less than 0.1 μm, secondary organic carbon, sea salt with a dry radius less than 0.2 μm, black carbon, and organic carbon; dry radius thresholds are chosen to ensure the aerosol size is less than 2.5 μm when water content is included) in the current-day simulation with the U.S. Air Quality System (USAQS) PM$_{2.5}$ observations.

[8] Our current-day simulation is designed to represent the climatological mean situation during 1981–2000. We thus evaluate the simulated summer mean and seasonal cycle of PM$_{2.5}$ with observations from the U.S. Air Quality System (AQS) averaged from 1997 (the earliest year with PM$_{2.5}$ data reported) through 2007. The simulated summer mean PM$_{2.5}$ is spatially correlated with the AQS observations ($R \sim 0.7$, over the Northeastern United States) with an average bias of 34% (Supporting Information, Figure S2). The positive bias occurs mainly over the Northeastern United States, where sulfate aerosol contributes above 50% to PM$_{2.5}$ in the model. This bias is expected since the simulation applies emissions for the year 1990 throughout the 20-year simulation (to minimize climate noise; section 2.1) but U.S. emissions of sulfur dioxide (SO$_2$, precursor to sulfate aerosol) decreased by about 30% from 1990 to 2000 [*EPA*, 2001], and this decrease should be reflected in the 1997–2007 AQS observations. The model exaggerates the seasonal cycle of simulated PM$_{2.5}$ over the Northeastern United States, likely due to excessive SO$_2$ emissions and subsequent sulfate production, but captures the summertime maximum (Supporting Information, Figure S3) which reflects stronger chemical production of aerosols during this season.

3. Representing the PM$_{2.5}$ Distribution with a Synthetic Tracer (SAt)

[9] The daily time series of SAt correlates strongly with PM$_{2.5}$ during summer ($R = 0.86$ for all 20 summers and $R = 0.8 – 0.9$ during individual summers). The cumulative density functions (CDFs) of daily mean surface concentrations of SAt and PM$_{2.5}$ for current-day and future climate conditions over the Northeastern United States (NEUS) suggest that both PM$_{2.5}$ and SAt have higher values at the high and low tails than a normal distribution (Figures 1a and 1b). Over the 10–98 percentile range, the SAt and PM$_{2.5}$ distributions are similar (Figure 1c). In the warmer climate, the mean summer PM$_{2.5}$ concentration increases by 15% (from 20 μg/m^3) from the current day to the future simulation, while the SAt concentration increases similarly, by 16%. Both distributions indicate an increase, especially at the upper tail of the distribution.
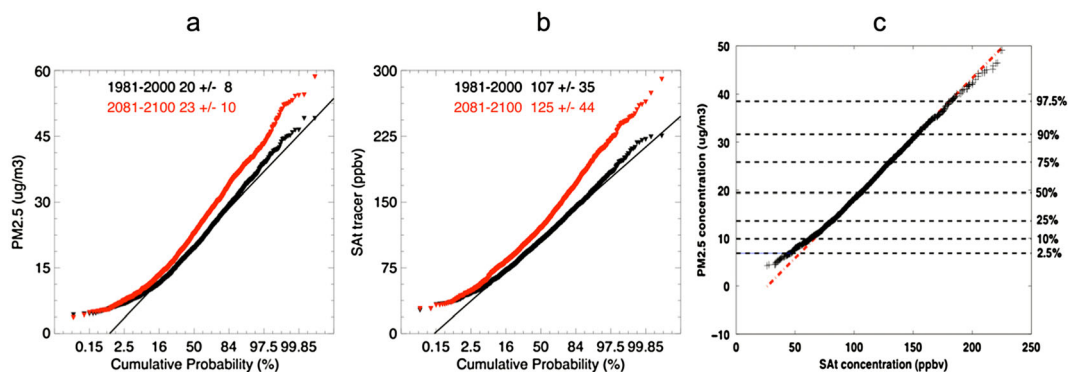
Figure 1. Cumulative density functions of summertime (a) daily PM$_{2.5}$ and (b) a SAt tracer with 25-day chemical lifetime and wet deposition in the GFDL AM3 current-day (black) and future (red) simulations. Each distribution is constructed from 92 summer daily average values over the U.S. Northeast region (36–46 N, 70–80 W, land only, 15 grid cells total, see Figure S2 in the Supporting Information) times 20 years each for 1990 and 2090 climate conditions. The numbers in the panels correspond to the mean and standard deviation of the distributions; the black solid line indicates a normal distribution with the same mean and standard deviation of PM$_{2.5}$ (in Figure 1a) and SAt tracer (in Figure 1b). (c) Quantile-quantile plot of summer daily SAt and PM$_{2.5}$ concentrations. Red line is the reference showing the same distribution. Dashed black lines indicate PM$_{2.5}$ at 2.5, 10, 25, 50, 75, 90, and 97.5% quantiles.

Concentrations at the upper tail (above 75%, representing pollution episodes) increase by 19% and 15% in the future climate for SAt and PM$_{2.5}$, respectively, while the increases at the lower tail (below 10%) only increase by 12% and 10%. The change from the current day to the future is statistically significant ($p < 0.01$, assessed by Kolmogorov-Smirnov test) for both SAt and PM$_{2.5}$. The stronger increase in the upper tail, which occurs for both SAt and PM$_{2.5}$, is consistent with the findings of *Mickley et al.* [2004] that climate change may increase high pollution episodes more strongly than mean pollution levels. As SAt is only affected by changing transport and precipitation in a changing climate, this higher tail increase is driven by changes in those two factors. Decreasing cyclones (hence increased stagnation, consistent with *Mickley et al.* [2004]) and decreasing frequencies of precipitations (especially of low-intensity precipitation, as in *Fang et al.* [2011]) are the major drivers for the higher tail increase. The strong correlation of daily average SAt and PM$_{2.5}$ and similarity of their CDFs suggest that the day-to-day variations of PM$_{2.5}$ are mainly driven by transport and removal and that SAt may be used as an index to reconstruct PM$_{2.5}$ and its changes in a warmer climate.

3.1. Linear Regression Model to Reconstruct PM$_{2.5}$ from SAt

[10] The strong correlation between PM$_{2.5}$ and SAt motivates us to examine the extent to which we can use a linear regression model to reconstruct daily PM$_{2.5}$ concentrations from daily SAt concentrations, i.e., $C_{PM2.5} = a + b * C_{SAt}$. Applying daily current-day summer concentrations of SAt and PM$_{2.5}$ in the AM3 simulations, we derive the coefficients: $a = -1.6$ (-0.8, -2.5) $\mu g/m^3$ and $b = 0.20$ (0.20, 0.21) $\mu g/m^3$ per ppbv (with numbers in the brackets indicating the 99% confidence interval of these coefficients). The linear model captures the magnitude of the 20-summer mean PM$_{2.5}$ concentrations (19.8 $\mu g/m^3$ for the reconstruction versus 20.2 $\mu g/m^3$ for simulated PM$_{2.5}$) and also 74% of the total PM$_{2.5}$ daily variability under current climate conditions (Figure 2a). Comparison of daily time series further confirms the utility of this linear regression model in representing the daily time series of PM$_{2.5}$ concentration over the Northeastern United States

(Figure 2b). During days with PM$_{2.5}$ episodes, the reconstruction tends to underestimate simulated PM$_{2.5}$ (section 3.2).

[11] We apply the same method to SAt and PM$_{2.5}$ in the future simulation and derive similar coefficient values, i.e., $a = -1.2$ (-0.6, 2.2) $\mu g/m^3$ and $b = 0.20$ (0.19, 0.20) $\mu g/m^3$ per ppbv (with numbers in the brackets indicating the 99% confidence intervals of these coefficients), which confirms that this relationship between SAt and PM$_{2.5}$ derived from the current-day simulation is also robust under the future climate scenario. This equivalence implies that the SAt relationship derived from the current-day simulation offers a good representation of PM$_{2.5}$ even under climate change scenarios.

[12] We next use the coefficients of the current-day linear regression model along with future SAt, all that would be available from implementing the synthetic tracer in a physical climate model, to reconstruct future PM$_{2.5}$. The reconstructed values are biased less than 2% for the 20-summer mean PM$_{2.5}$ concentration and capture 80% of the AM3 simulated PM$_{2.5}$ daily variability in the future simulation (Figures 2c and 2d). The future change in mean PM$_{2.5}$ is also fairly well captured by applying the linear regression model (3.5 $\mu g/m^3$ increase in the linear regression model versus 3 $\mu g/m^3$, simulated by AM3). The PM$_{2.5}$ non-attainment days corresponding to the 35 $\mu g/m^3$ daily mean PM$_{2.5}$ standard are also well represented: 4% and 14% of all summer days are non-attainment days in AM3 present and future climate simulations, respectively; those statistics are 3% and 12% for the regression model.

3.2. Factors Leading to Underestimated SAt-derived PM$_{2.5}$ Values on Polluted Days

[13] Despite the high correlation between the SAt and PM$_{2.5}$ time series, Figures 2b and 2d show that the linear regression model slightly underestimates PM$_{2.5}$ concentrations relative to the AM3 simulation. We further examine these situations in the current-day simulation by comparing mean PM$_{2.5}$ and precipitation distributions on all summer days and on days when the bias between the simulated and reconstructed PM$_{2.5}$ exceeds 10 $\mu g/m^3$. The largest underestimates typically occur when PM$_{2.5}$ over the Northeastern
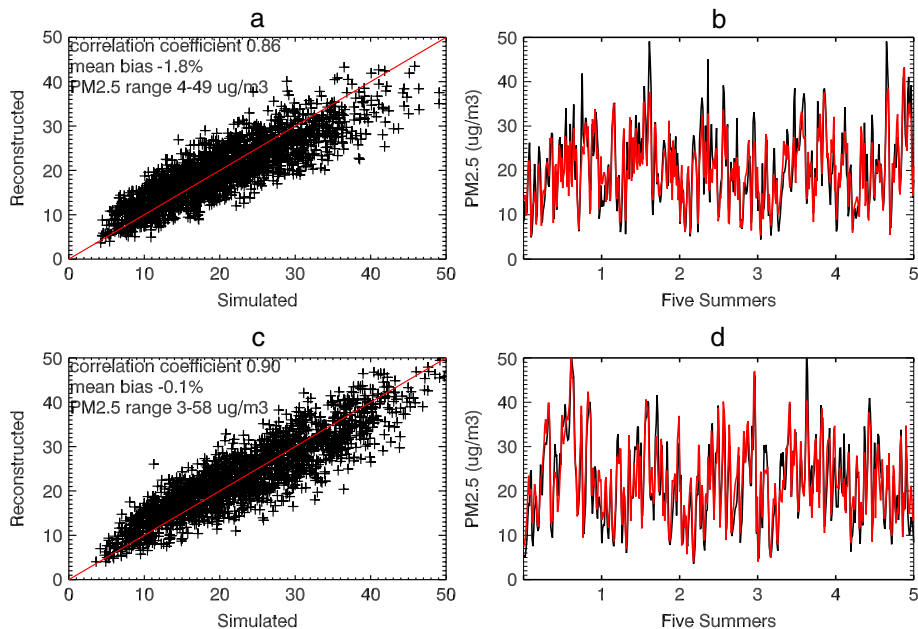
Figure 2. (a) Scatter plot of daily PM$_{2.5}$ as simulated by the GFDL AM3 model versus PM$_{2.5}$ as reconstructed by applying the linear regression model (section 3.1) to the SAt distribution over the Northeastern United States for the 20 summers with 1990 climate conditions (black plus signs). The red line shows the 1:1 relationship. (b) An example 5 year time series of simulated (black) and reconstructed (red) daily PM$_{2.5}$ concentrations over the Northeastern United States (unit: μg/m^3); (c and d) similar to Figures 2a and 2b, respectively, but with 2090 climate condition.

United States is larger than the summer average (by ~10 μg/m^3; Supporting Information, Figures S4a and S4b) and when precipitation is stronger than average (Figures S4c and S4d). Results are similar for composite plots from the future simulations (not shown).

[14] Further analysis indicates that these precipitation events are associated with pollution transport. For example, for one such episode, PM$_{2.5}$ transported from Kentucky and Tennessee enhances the PM$_{2.5}$ concentration over the Northeastern United States. Inspection of daily SAt distributions over the Eastern United States during this event reveals negligible contribution of transport from these regions to the SAt concentration over the Northeastern United States (Supporting Information, Figure S5) for two reasons. First, the SAt tracer emission follows CO; its source over Kentucky and Tennessee is much weaker compared to that of PM$_{2.5}$ precursors (SO$_2$, for example, Supporting Information, Figure S6). Second, the SAt tracer is soluble, while some components of PM$_{2.5}$ and its precursors, such as hydrophobic black carbon (BC) and organic carbon (OC), are not soluble. Consequently, on days with strong precipitation, SAt is removed more quickly than PM$_{2.5}$. These findings imply that the utility of SAt may be further improved by implementing two separate tracers: one with SO$_2$ emissions and sulfate solubility (as tested in section 4) and one with carbonaceous emissions and solubility.

3.3. Extension to Springtime and Other Regions

[15] To examine whether SAt can represent PM$_{2.5}$ over other polluted regions at northern midlatitudes, we analyze SAt and PM$_{2.5}$ daily time series for 20 summers over the Midwest United States (MWUS), Northern East Asia (NEEA), Southern East Asia (SEEA), Mediterranean Europe (MEU), and Northern Europe (NEU). In general, SAt is strongly correlated with PM$_{2.5}$ ($R = 0.71 \sim 0.89$), although

the regression slope varies by region (slope $= 0.19 \sim 0.31$), reflecting differences in regional budgets of PM$_{2.5}$ (Supporting Information, Table S1). As long as region-specific relationships (regression coefficients) are determined from a current-day simulation, future PM$_{2.5}$ can be reconstructed fairly well by using the current-day linear relationship between SAt and PM$_{2.5}$ along with the simulated future SAt tracer (Table S1). Over all regions, the mean bias in PM$_{2.5}$ is within $\pm7\%$ and about $50 \sim 80\%$ variability of daily PM$_{2.5}$ is captured.

[16] We further analyze the utility of SAt in spring (MAM) when long-range transport is relatively more important than during summer (e.g., *HTAP* [2010]). Over NEUS, MWUS, MEU, and NEU, simulated PM$_{2.5}$ and SAt are correlated in the current-day simulations slightly less than in summer ($R = 0.68 - 0.75$, Table S1). The reconstructed and simulated future PM$_{2.5}$ are also fairly well correlated ($R^2 \sim 0.5$), and the mean bias of this regression model is within $\pm10\%$ over these regions (Table S1). Over NEEA and SEEA, however, the springtime correlation is weak ($R^2 < 0.2$), indicating that the SAt tracer does not adequately represent PM$_{2.5}$. The poor applicability of SAt over SEEA and NEEA is associated with stronger long-range transport during spring. As shown in section 3.2, discrepancies in solubility and emissions between SAt and PM$_{2.5}$ precursors may accumulate during long-range transport, weakening the correlation between them. This problem is largely overcome by tying SAt to SO$_2$ rather than CO emissions (section 4). We conclude that synthetic tracers can be generally applied in climate models with similar success in representing PM$_{2.5}$ over several Northern Hemispheric regions in spring and summer.

4. Sensitivity of Tracer Representation to Different Current-day Meteorology and Emissions

[17] Prior to implementing synthetic tracers for air quality applications in physical climate models, we need to

determine the extent to which the relationship between PM$_{2.5}$ and SAt depends on model configuration. As a preliminary step, we analyze here a different version of the GFDL AM3 model in which the meteorology is nudged to National Centers for Environmental Prediction (NCEP) reanalysis winds as described by *Lin et al.* [2012a, 2012b] for the time period of 1979–2010 and thus is comparable to a chemical transport model. This simulation includes the same SAt tracer and applies annually invariant emissions of air pollutants during 1979–2010. Despite the different setting of AM3 nudged simulations, its SAt and PM$_{2.5}$ are still strongly correlated with similar correlation coefficients ($R = 0.71 \sim 0.85$, Supporting Information, Table S2). The slopes, which are applied to the reconstruction, however, slightly vary due to differences in the emission inventory used (the nudged version uses climatological mean emissions from 1979 to 2010 [*Lin et al.*, 2012b], while the interactive version uses emissions representing 1990 levels [*Fang et al.*, 2011]).

[18] We further use this simulation to explore whether we can improve the SAt performance over regions where sulfate dominates total PM$_{2.5}$ by tying the emissions to SO$_2$. For this purpose, we implement a second synthetic tracer, denoted SO2t, which is the same as SAt except the CO emissions are replaced by SO$_2$ emissions. Given the larger molar emission rate of CO versus SO$_2$ (global emissions of SO$_2$ and CO are approximately 2 versus 44 T mol per year, respectively) and hence more abundant SAt than SO2t in the atmosphere, the slope of the regression model of SO2t is larger than that for SAt in summer (slope = $1.54 \sim 2.25$, Table S2). A strong linear correlation emerges for both the SO2t and SAt tracers and PM$_{2.5}$ over all regions ($R = 0.71 \sim 0.91$, Table S2). The linear correlation between SO2t and PM$_{2.5}$ is stronger than that between SAt and PM$_{2.5}$ over all regions chosen, consistent with our hypothesis in section 3.2. During spring, the improvement is particularly large over NEEA and SEEA, where the correlation coefficients between tracers and PM$_{2.5}$ increase from 0.39 and 0.40 (using SAt and PM$_{2.5}$) to 0.73 and 0.72 (using SO2t and PM$_{2.5}$).

5. Conclusions

[19] We implement a simple soluble synthetic aerosol tracer (SAt; tied to CO emissions) in the GFDL AM3 coupled chemistry-climate model [*Donner et al.*, 2011] and show that it correlates strongly ($R = 0.86$) with day-to-day variations in simulated surface PM$_{2.5}$ concentrations over the Northeastern United States. With a simple linear regression model that uses SAt to reconstruct PM$_{2.5}$, we show that this tracer can represent the response of the regional PM$_{2.5}$ distribution to climate change. Specifically, the PM$_{2.5}$ distribution reconstructed from SAt captures around 80% of the daily variability, the magnitude of regional mean PM$_{2.5}$, and the incidence PM$_{2.5}$ non-attainment days, and their changes from the current-day distribution over several Northern Hemispheric regions in both spring and summer (Table S1; Figures 1 and 2). The tracer is similarly accurate when applied in AM3 with a different configuration (meteorology and emissions; Table S2). Our proof-of-concept study demonstrates that, as long as the model-specific regression coefficients are determined from a full-chemistry simulation for a current-day scenario, future PM$_{2.5}$ can be reconstructed

by applying the current-day linear relationship between synthetic tracers and PM$_{2.5}$ to the simulated future synthetic tracer at least on regional scales (as seen from AM3 in Table S1). Further refinements may improve the utility of synthetic tracers over specific regions of interest (e.g., tracers designed for sulfate, carbonaceous aerosols, or dust).

[20] Future chemistry-climate multimodel ensemble projects could include synthetic tracers (as in *HTAP* [2010]) to evaluate whether model-independent relationships between tracers and PM$_{2.5}$ can be developed. Such an effort is an essential step towards eliminating the need for model-specific regression coefficients to be determined from a current-day full-chemistry simulation. Our method would then be an easy-to-implement and low-cost addition to state-of-the-art physical climate models, such as those routinely run in centuries long "production" simulations for assessment reports at international modeling centers. Trade-offs between increasing spatial resolution, important for representing smaller scale processes and additional process-level complexity, such as full representation of atmospheric chemistry, are inevitable. Implementing such a tracer into high-resolution physical climate models would expand the number of scenarios and simulation years available to assess multimodel air quality projections, allowing air quality managers to reap the benefits of these models—which would otherwise not be possible in the absence of fully coupled chemistry.

References

Appelhans, T., A. Sturman, and P. Zawar-Reza (2012), Synoptic and climatological controls of particulate matter pollution in a Southern Hemisphere coastal city, *Int. J. Climatol.*, doi:10.1002/joc.3439.

Bey, I., D. J. Jacob, J. A. Logan, and R. M. Yantosca (2001), Asian chemical outflow to the Pacific in spring: Origins, pathways, and budgets, *J. Geophys. Res.*, *106*(D19), 23,097–23,113.

Cooper, O. R., J. L. Moody, D. D. Parrish, M. Trainer, T. B. Ryerson, J. S. Holloway, G. H. bler, F. C. Fehsenfeld, S. J. Oltmans, and M. J. Evans (2001), Trace gas signatures of the airstreams within North Atlantic cyclones: Case studies from the North Atlantic Regional Experiment (NARE '97) aircraft intensive, *J. Geophys. Res.*, *106*(D6), 5437–5456.

Dockery, D. W., C. A. Pope, X. Xu, J. D. Spengler, J. H. Ware, M. E. Fay, B. G. Ferris, and F. E. Speizer (1993), An association between air pollution and mortality in six U.S cities. *New England Journal of Medicine*, *329*(24), 1753–1759.

Donner, L. J., et al. (2011), The dynamical core, physical parameterizations, and basic simulation characteristics of the atmospheric component AM3 of the GFDL Global Coupled Model CM3, *J. Clim.*, (*24*), 3484–3519.

EPA (2001), Latest findings on national air quality: 2000 status and trends, United States, Environmental Protection Agency, EPA 454/K-01-002, http://www.epa.gov/airtrends/aqtrnd00/brochure/00brochure.pdf.

Fang, Y., A. M. Fiore, L. W. Horowitz, A. Gnanadesikan, I. Held, G. Chen, G. Vecchi, and H. I. Levy (2011), The impacts of changing transport and precipitation on pollutant distributions in a future climate, *J. Geophys Res.*, 116.

Fiore, A. M., et al. (2012), Global air quality and climate, *Chem. Soc. Rev.*, doi:10.1039/C2CS35095E.

HTAP (2010), Hemispheric Transport of Air Pollution 2010, United Nations, New York, Geneva

HTAP (2007), Hemispheric Transport of Air Pollution 2007, United Nations, New York, Geneva

Jacob, D. J., and D. A. Winner (2009), Effect of climate change on air quality, *Atmos. Environ.*, *43*(1), 51–63.

Kloster, S., F. Dentener, J. Feichter, F. Raes, U. Lohmann, E. Roeckner, and I. Fischer-Bruns (2010), A GCM study of future climate response to aerosol pollution reductions, *Clim. Dynam.*, *34*(7), 1177–1194.

Lin, M., et al. (2012a), Transport of Asian ozone pollution into surface air over the Western United States in spring, *J. Geophys. Res.*, *117*, D00V07, doi:10.1029/2011JD016961.

Lin M., et al. (2012b), Springtime high surface ozone events over the Western United States: Quantifying the role of stratospheric intrusions, *J. Geophys. Res.*, *117*, D00V22, doi:10.1029/2012JD018151.

Liu, J., D. L. Mauzerall, and L.W. Horowitz, (2005), Analysis of seasonal and interannual variability in transpacific transport, *J. Geophys. Res.*, *110*, D04302, doi:10.1029/2004JD005207.

Meehl, G. A., et al. (2007), Global Climate Projections, in *Climate Change 2007*: *The Physical Science Basis. Contribution of Working Group I to the Fourth Assessment Report of the Intergovernmental Panel on Climate Change*, edited by S. Soloman, D. Qin, M. Manning, M. Marquis, K. Averyt, M. M. B. Tignor, H. J. Miller, and Z. Chen, pp. 747–845, Cambridge University Press.

Mickley, L. J., D. J. Jacob, B. D. Field, and D. Rind (2004), Effects of future climate change on regional air pollution episodes in the United States, *Geophys. Res. Lett.*, *31*(L24103).

Park, R. J., D. J. Jacob, N. Kumar, and R. M. Yantosca (2006), Regional visibility statistics in the United States: Natural and trans-boundary pollution influences, and implications for the Regional Haze Rule, *Atmos. Environ.*, *40*(28), 5405–5423.

Parry, M. L., O. F. Canziani, J. P. Palutikof, P. J. van der Linden, and C. E. Hanson (2007), Impacts, Adaptation, and Vulnerability. Contribution of Working Group II to the Fourth Assessment Report of the Intergovernmental Panel on Climate Change, 2007, Cambridge University Press, Cambridge, United Kingdom and New York, NY, USA.

Pope, C. A., and D. W. Dockery (2006), Health effects of fine particulate air pollution: Lines that connect, *J. Air Waste Manage. Assoc.*, *56*(6), 709–742.

Pope, C. A., R. T. Burnett, M. J. Thun, E. E. Calle, D. Krewski, K. Ito, and G. D. Thurston (2002), Lung cancer, cardiopulmonary mortality, and long-term exposure to fine particulate air pollution, *JAMA*, *287*(9), 1132–1141.

Pope, C. A. (2000), Invited commentary: Particulate matter-mortality exposure-response relations and threshold, *Am. J. Epidemiol.*, *152*(5), 407–412.

Schultz, M., and S. Rast (2007), Emission datasets and methodologies for estimating emissions, available at: http://retro.enes.org/reports/D1-6_final.pdf.

Schwartz, J., F. Laden, and A. Zanobetti (2002), The concentration-response relation between PM$_{2.5}$ and daily deaths, *Environ. Health Perspect.*, *110*(10).

Staudt, A. C., D. J. Jacob, J. A. Logan, D. Bachiochi, T. N. Krishnamurti, and G. W. Sachse (2001), Continental sources, transoceanic transport, and interhemispheric exchange of carbon monoxide over the Pacific, *J. Geophys. Res.*, *106*(D23), 32,571–32,589.

Shindell D. T., et al. (2008), A multi-model assessment of pollution transport to the Arctic, *Atmos. Chem. Phys.*, *8*, 5353–5372, doi:10.5194/acp-8-5353-2008.

Stohl, A., S. Eckhardt, C. Forster, P. James, and N. Spichtinger (2002), On the pathways and timescales of intercontinental air pollution transport, *J. Geophys. Res.*, *107*(D23), 4684.

Tai, A. P. K., L. J. Mickley, and D. J. Jacob, (2012), Impact of 2000–2050 climate change on fine particulate matter (PM2.5) air quality inferred from a multi-model analysis of meteorological modes, *Atmos. Chem. Phys. Discuss.*, *12*, 18,107–18,131, doi:10.5194/acpd-12-18107-2012.

Textor, C., et al. (2006), Analysis and quantification of the diversities of aerosol life cycles within AeroCom, *Atmos. Chem. Phys.*, *6*(7), 1777–1813.

van der Werf, G. R., et al. (2006), Interannual variability in global biomass burning emissions from 1997 to 2004, *Atmos. Chem. Phys.*, *6*, 3423–3441, doi:10.5194/acp-6-3423-2006.